AMERICAN SOCIETY FOR MICROBIOLOGY | Journal of Virology®

VIRUS-CELL INTERACTIONS

Fragile X-Related Protein FXR1 Controls Human Adenovirus Capsid mRNA Metabolism

Zamaneh Hajikhezri,[a] Yanina Kaira,[a] Erik Schubert,[a] Mahmoud Darweesh,[a,b] Catharina Svensson,[a] Göran Akusjärvi,[a] Tanel Punga[a]

[a]Department of Medical Biochemistry and Microbiology, Uppsala University, Uppsala, Sweden
[b]Department of Microbiology and Immunology, Faculty of Pharmacy, Alazhr University, Assiut, Egypt

ABSTRACT Human adenoviruses (HAdVs) are widespread pathogens causing a variety of diseases. A well-controlled expression of virus capsid mRNAs originating from the major late transcription unit (MLTU) is essential for forming the infectious virus progeny. However, regulation of the MLTU mRNA metabolism has mainly remained enigmatic. In this study, we show that the cellular RNA-binding protein FXR1 controls the stability of the HAdV-5 MLTU mRNAs, as depletion of FXR1 resulted in increased steady-state levels of MLTU mRNAs. Surprisingly, the lack of FXR1 reduced viral capsid protein accumulation and formation of the infectious virus progeny, indicating an opposing function of FXR1 in HAdV-5 infection. Further, the long FXR1 isoform interfered with MLTU mRNA translation, suggesting FXR1 isoform-specific functions in virus-infected cells. We also show that the FXR1 protein interacts with N6-methyladenosine (m^6A)-modified MLTU mRNAs, thereby acting as a novel m^6A reader protein in HAdV-5 infected cells. Collectively, our study identifies FXR1 as a regulator of MLTU mRNA metabolism in the lytic HAdV-5 life cycle.

IMPORTANCE Human adenoviruses (HAdVs) are common pathogens causing various self-limiting diseases, such as the common cold and conjunctivitis. Even though adenoviruses have been studied for more than 6 decades, there are still gaps in understanding how the virus interferes with the host cell to achieve efficient growth. In this study, we identified the cellular RNA-binding protein FXR1 as a factor manipulating the HAdV life cycle. We show that the FXR1 protein specifically interferes with mRNAs encoding essential viral capsid proteins. Since the lack of the FXR1 protein reduces virus growth, we propose that FXR1 can be considered a novel cellular proviral factor needed for efficient HAdV growth. Collectively, our study provides new detailed insights about the HAdV-host interactions, which might be helpful when developing countermeasures against pathogenic adenovirus infections and for improving adenovirus-based therapies.

KEYWORDS FXR1, adenovirus, m6A-modification, mRNA decay, mRNA translation

Human adenoviruses (HAdVs) are widespread pathogens causing ocular, respiratory, and gastrointestinal diseases (1, 2). Essential for HAdV pathogenesis is a temporally ordered viral gene expression. The early genes (e.g., E1A, E1B, E2, E3, E4) have individual transcription units and encode proteins involved in the suppression of the host cell response, deregulation of the cell cycle, and inducing virus DNA replication (3–5). In contrast, almost all HAdV late genes are expressed from a single transcription unit, the major late transcription unit (MLTU). The HAdV-5 MLTU encodes a 27,000-nucleotide-long major late pre-mRNA. Five families of viral mRNAs (the L1 to L5 mRNAs; Fig. 1A) are generated through alternative polyadenylation (6). These transcripts are further processed by alternative pre-mRNA splicing into multiple mature MLTU mRNAs (6–8). Even though there is an enormous accumulation of various alternatively

Editor Colin R. Parrish, Cornell University Baker Institute for Animal Health

Address correspondence to Tanel Punga, Tanel.Punga@imbim.uu.se.

The authors declare no conflict of interest.

Received 17 October 2022
Accepted 18 January 2023
Published 7 February 2023

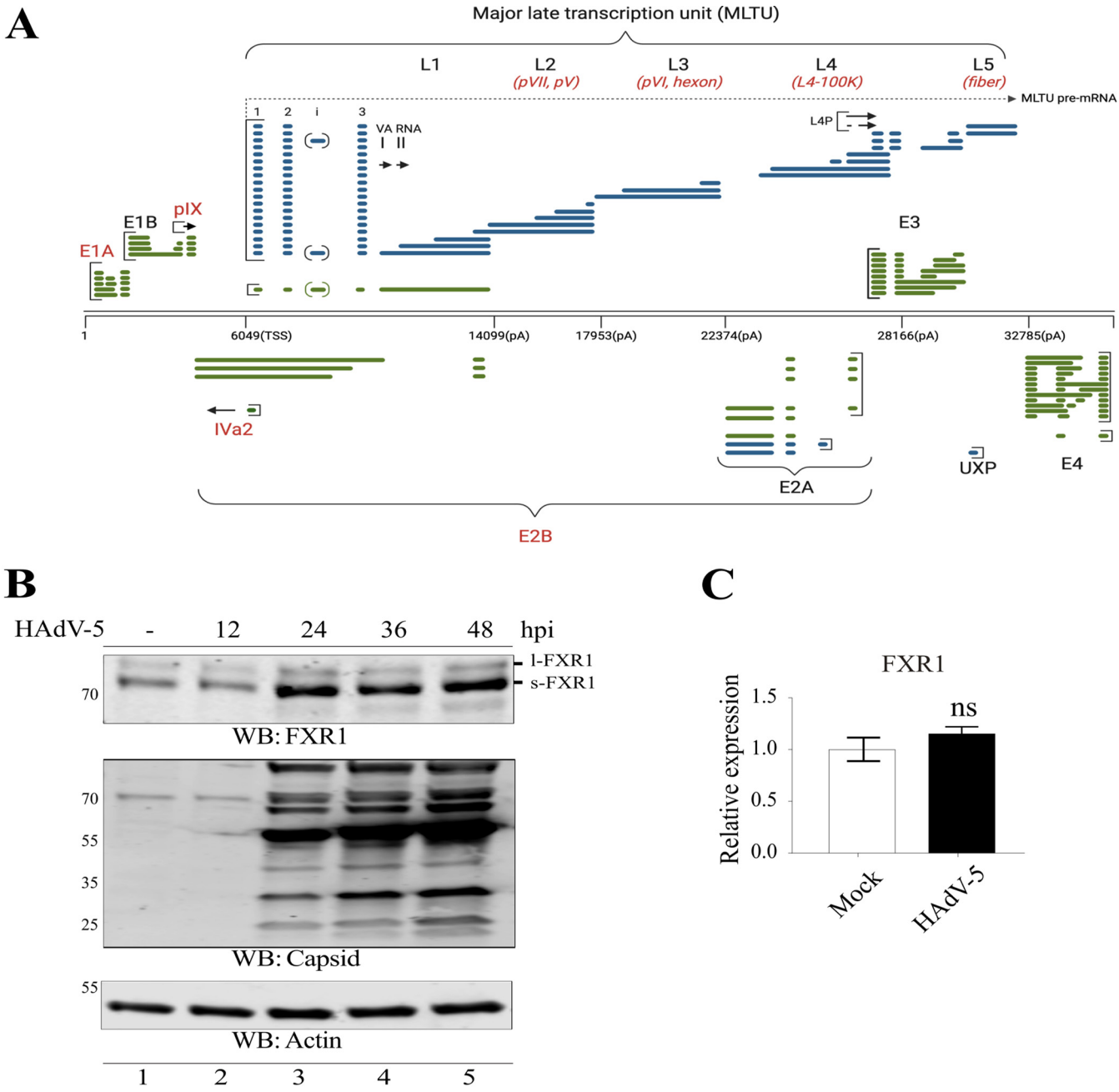

FIG 1 The FXR1 protein accumulates during the late phase of a HAdV-5 infection. (A) Schematic overview of the HAdV-5 genome and transcription units. Modified from reference 8, the image was created with BioRender.com. Early (green) and late (blue) expressed genes are indicated, and genes analyzed in the present study are shown in red. Three tripartite leader exons are indicated with numbers (1 to 3). The numbers below the double line represent the HAdV-5 nucleotides marking the MLTU transcription start site (TSS) and known polyadenylation signals (pA) based on reference 6. (B) The FXR1 protein accumulates in HAdV-5-infected HeLa cells. Cells were harvested at the indicated hours postinfection (hpi). Proteins were detected with Western blotting (WB) using the anti-FXR1, anti-HAdV capsid, and anti-actin antibodies. Short (s-FXR1) and long (l-FXR1) FXR1 isoforms are indicated. (C) FXR1 mRNA accumulation. qRT-PCR data are shown as the relative expression of the FXR1 mRNA in noninfected (mock) and HAdV-5-infected (MOI, 5) HeLa cells at 24 hpi. The FXR1 primers used do not discriminate between s-FXR1 and l-FXR1 mRNAs. Bars represent relative FXR1 expression (mean ± standard deviation [SD]) after normalization to the GAPDH mRNA; ns, nonsignificant.

processed and modified MLTU transcripts during infection (6–8), only a fraction encode proteins with well-established functions. Almost all these proteins are viral structural proteins, collectively known as the capsid proteins (9).

Processing of the MLTU transcripts is under rigorous control mechanisms involving both viral and cellular proteins. This includes the viral E4orf4 and L4-33K and the cellular PP2A and p32/C1QBP proteins, which regulate alternative splicing of the L1 family

mRNAs in a temporal manner during the virus life cycle (10–15). Virus pre-mRNA processing is further influenced by the cellular RNA-binding proteins RALY and hnRNP-C, which inhibit virus MLTU mRNA splicing in infected cells (16). In addition to the processing by polyadenylation and splicing, many MLTU transcripts undergo N6-methyladenosine (m^6A) modifications (7). A recent study has shown that the cellular m^6A writer enzyme METTL3 specifically modifies the MLTU transcripts, such as the fiber (L5) pre-mRNA, and thereby controls its splicing efficiency (7).

Fragile X mental retardation protein 1 (FXR1) is a multifunctional RNA-binding protein involved in different steps of posttranscriptional gene regulation (17, 18). The FXR family of proteins also includes the highly homologous fragile X messenger ribonucleoprotein 1 (FMR1) and FMR1 autosomal homolog 2 (FXR2) proteins (19). All the family members share significant structural similarities by containing two Tudor domains, the K homology (KH) domains, and an arginine-glycine-glycine repeat (RGG) (20, 21). FXR1 is a cytoplasmic RNA-binding protein with the best-known function as an mRNA translation regulator (22–24). In addition, the FXR1 protein has been implicated in regulating transcription, mRNA transport, and mRNA stability (25–28).

Alternative splicing of the FXR1 pre-mRNA generates a variety of FXR1 protein isoforms in murine and human cells (19, 29). Since the FXR1 isoform nomenclature is perplexing, we refer to the two human FXR1 proteins studied in the present report as the short FXR1 (s-FXR1) and long FXR1 (l-FXR1) based on the length of their C-terminal intrinsically disordered domain (IDD) (see below). The abundant s-FXR1 (539 amino acids, also known as human isoform B, FXR1a, transcript variant 2) has been characterized as an RNA-binding protein regulating translation and cell migration (22, 24, 28). The biological role of l-FXR1 (621 amino acids, also known as isoform A) is less well characterized, although it has been shown to specifically regulate cell proliferation (26).

Since most MLTU mRNAs accumulate at high levels in infected cells, different RNA-binding proteins likely control their synthesis and stability. However, there is limited knowledge about the cellular RNA-binding proteins involved in these processes. Therefore, the present study aimed to elucidate if and how the known RNA-binding protein FXR1 interferes with HAdV-5 MLTU mRNA metabolism.

RESULTS

The FXR1 protein accumulates during the late phase of a HAdV-5 infection. HAdV type 5 (HAdV-5) early and late gene transcripts undergo extensive processing to achieve a temporal expression pattern in the infected cells (Fig. 1A). In search for potential cellular RNA-binding proteins targeting HAdV-5 transcripts, we analyzed the available HAdV-2 proteomics data sets for proteins showing an upregulation during infection (30, 31). This search strategy was based on our previous study, where we showed that upregulation of the cellular RNA-binding protein ZC3H11A correlated with an efficient nuclear export of the HAdV-5 fiber mRNA, a member of the MLTU L5 family (32). Among the different upregulated RNA-binding proteins, our attention was caught by the FXR1 protein (30). To investigate whether HAdV-5 impacts FXR1, we analyzed the FXR1 protein accumulation in virus-infected HeLa cells. HAdV-5 was chosen as it is highly similar to HAdV-2 (95% homology at the genome level) and due to our previous studies with this particular virus type (32–35). As shown in Fig. 1B, the FXR1 protein exhibited increased accumulation starting at 24 h postinfection (hpi) (lanes 3 to 5) when also the late phase of infection commenced (capsid protein staining as the read-out). Notably, accumulation was more prominent for the s-FXR1 isoform than for the l-FXR1 isoform in HeLa cells. This increase was not due to enhanced FXR1 gene transcription, as total FXR1 mRNA levels did not change considerably at 24 hpi (Fig. 1C).

Taken together, these data indicate that HAdV-5 infection causes an upregulation of the FXR1 protein during the late phase of infection.

FXR1 deficiency affects virus capsid protein accumulation and reduces the formation of infectious progeny. Since the endogenous FXR1 protein accumulated during infection (Fig. 1B), we hypothesized that FXR1 might have an essential role during HAdV-5 infection. To this end, we used the CRISPR/Cas9 genome editing approach

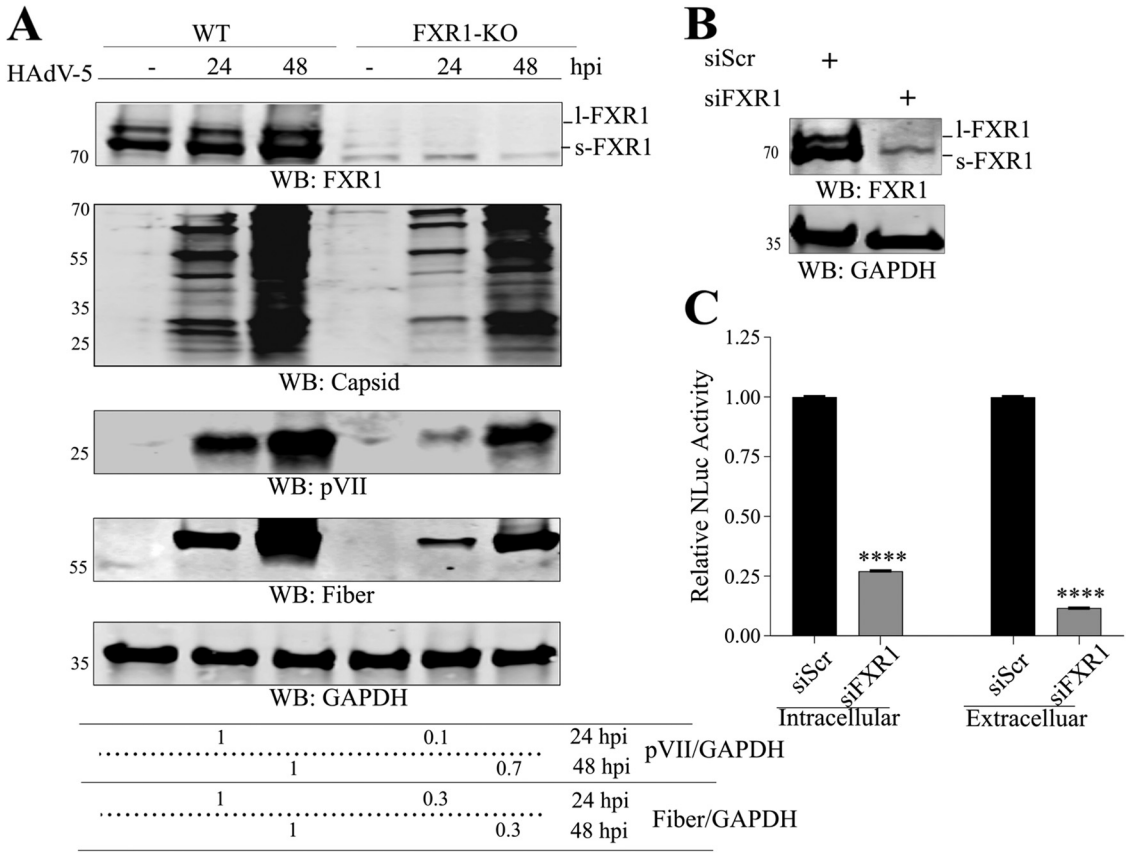

FIG 2 FXR1 deficiency affects HAdV-5 capsid protein accumulation and reduces the formation of infectious progeny. (A) Unmodified A549 (WT, expressing Cas9) and CRISPR/Cas9-modified A549 (FXR1-KO) cells were infected with HAdV-5 (24 hpi), and the proteins were detected with WB using the anti-FXR1, anti-capsid, anti-pVII (L2), anti-fiber (L5), and anti-GAPDH antibodies. (B) WB shows the efficiency of the FXR1 siRNA (siFXR1) in HeLa cells. siScr, scrambled siRNA. (C) Reduced formation of the infectious virus particles in the siFXR1-treated cells. Cell lysates (intracellular virus) or cell growth medium (extracellular virus) from siRNA-treated and Ad5-Luc3 virus-infected HeLa cells were used to reinfect fresh HeLa cells. The enzymatic activity of the luciferase (Luc) protein was used to measure virus infectivity. Data (mean ± SD) are shown as relative luciferase activity after considering the siScr sample as 1; ****, $P < 0.0001$.

to generate an FXR1 knockout A549 cell line (FXR1-KO). The control (wild type [WT], transfected with the Cas9 protein-expressing plasmid) and FXR1-KO cells were infected with HAdV-5, and accumulation of the viral capsid proteins was monitored as the read-out of productive virus growth. The virus capsid proteins, among them the essential fiber (L5) and pVII (L2) proteins, showed reduced accumulation in the FXR1-KO cells compared to the control A549 (WT) cells (Fig. 2A). Reduced capsid protein amount should affect the formation of infectious virus particles. To test this, HeLa cells were treated with FXR1-specific small interfering RNA (siRNA) (siFXR1) (Fig. 2B), followed by infection with the replication-competent Ad5-Luc3 virus expressing the luciferase reporter gene (36). The cell lysates (i.e., intracellular virus, read-out of particle formation) and cell culture supernatants (i.e., extracellular virus, read-out of particle release) from siScr- or siFXR1-treated and Ad5-Luc3-infected cells were used to reinfect HeLa cells. Quantification of the luciferase activity was used to measure infectious virus particles in the reinfected HeLa cells. If the lack of FXR1 affected infectious progeny, it should correlate with reduced luciferase activity in the reinfected cells. Indeed, both intracellular virus and extracellular reporter virus signals were significantly decreased in the siFXR1-treated cells compared to the siScr-treated cells (Fig. 2C). We have used the knockdown approach in the HeLa cell because siRNA treatments worked better (i.e., knockdown efficiency was best) in this cell line, whereas specific CRISPR/Cas9 editing at the FXR1 locus was only achieved in A549 cells. Another reason for using both experimental approaches was to avoid potential off-target effects caused either by siRNA or CRISPR/Cas9.

Overall, our data indicate that FXR1 is needed for the accumulation of the capsid proteins and the efficient formation of infectious virus particles.

FXR1 protein elimination increases the stability of the MLTU mRNAs. Considering that FXR1 deficiency affected viral capsid protein accumulation (Fig. 2A), we hypothesized that FXR1 might specifically target the viral capsid mRNAs (i.e., MLTU). Surprisingly, all tested MLTU transcripts showed enhanced, and not reduced, accumulation in the A549 FXR1-KO cells compared to the control cells (Fig. 3A). The tested MLTU mRNAs (pV [L2], pVII [L2], hexon [L3], L4-100K [L4], fiber [L5]) also showed an enhanced accumulation in the siFXR1-treated HeLa cells (Fig. 3B). Overall, FXR1 seems to specifically target MLTU transcripts, as the viral early/intermediate E1A, E2B, and pIX mRNAs were not considerably affected (Fig. 3A and 3B).

FXR1 can regulate the stability of specific transcripts (27). Therefore, increased MLTU mRNA steady-state levels might be due to increased mRNA stability. To test this hypothesis, mRNA levels were monitored in siFXR1-treated and HAdV-5-infected HeLa cells following inhibition of RNA synthesis with actinomycin D (ActD). Notably, increased stability of some MLTU mRNAs in siFXR1-treated cells was observed (Fig. 3C). In particular, the mRNAs originating from the L2 (pV, pVII) and L5 (fiber) regions (Fig. 1A) were resistant to degradation in siFXR1-treated cells. Virus mRNAs originating from the early (E2B), intermediate (pIX), or late (L3; hexon, L4; L4-100K) did not show increased stability in FXR1 knockdown cells (Fig. 3C). An exception was viral intermediate IVa2 transcript, which accumulated specifically in the siFXR1-treated HeLa cells. Accumulation of the cellular peroxisome proliferator-activated receptor-α (PPARα) mRNA, the stability of which is not regulated by FXR1 (27), was not altered in the siFXR1-treated cells, hence supporting the specificity of our experiment.

Since FXR1 is an RNA-binding protein, we tested whether the FXR1 protein can bind to MLTU mRNAs. For this experiment, an RNA cross-linking-immunoprecipitation in virus-infected HeLa cells, followed by reverse transcriptase quantitative PCR (RT-qPCR; CLIP-qPCR), was performed. Immunoprecipitation of the endogenous FXR1 protein showed a striking enrichment of the MLTU mRNAs and some enrichment of the IVa2 mRNA (Fig. 3D). Quantification of the data revealed that the FXR1 protein did not bind to the early/intermediate E1A, E2B, and pIX mRNAs in the same experiment (Fig. 3D).

Taken together, our results suggest that the FXR1 protein preferably binds to and regulates the stability of MLTU mRNAs.

Different roles of the s-FXR1 and l-FXR1 proteins in MLTU mRNA metabolism. Alternative splicing of human FXR1 pre-mRNA generates the s-FXR1 and l-FXR1 isoforms with different lengths of the C-terminal IDD (Fig. 4A) (37). To test how these isoforms target MLTU mRNAs, we generated three A549 FXR1-KO cell lines transduced either with a non-FXR1 expressing lentivirus (referred to as "control") or with the lentiviruses encoding the Flag-s-FXR1 or Flag-l-FXR1 proteins. The l-FXR1 protein expression increased the pVII and fiber protein accumulation in virus-infected cells (Fig. 4B). In contrast, the s-FXR1 did not considerably affect the fiber protein accumulation. Quantitative analysis of the Western blot indicated that although s-FXR1 did not increase the fiber protein level, it still raised the pVII protein levels to some extent (Fig. 4B). Since FXR1 controls MLTU mRNA stability (Fig. 3C), pVII and fiber mRNA accumulation was tested in the same lentivirus-transduced cell lines. As shown in Fig. 4C, fiber and pVII mRNA levels did not increase in s-FXR1- or l-FXR1-expressing cells. Notably, expression of the s-FXR1 protein seems to have a more general effect on mRNA metabolism, as its expression affected the accumulation of all tested (E2B, pVII, fiber) viral mRNAs. To validate the RNA-binding specificity of the FXR1 isoforms, we performed the CLIP-qPCR experiment in the same lentivirus-transduced A549 FXR1-KO cell lines. Interestingly, only the Flag-l-FXR1 protein interacted specifically with the pVII and fiber mRNAs, whereas its binding to early E2B mRNA was not detected (Fig. 4D). The s-FXR1 isoform showed essentially no binding to the tested mRNAs.

Together, our results indicate that l-FXR1 specifically targets pVII and fiber mRNAs and enhances the expression of these two viral proteins in A549 cells.

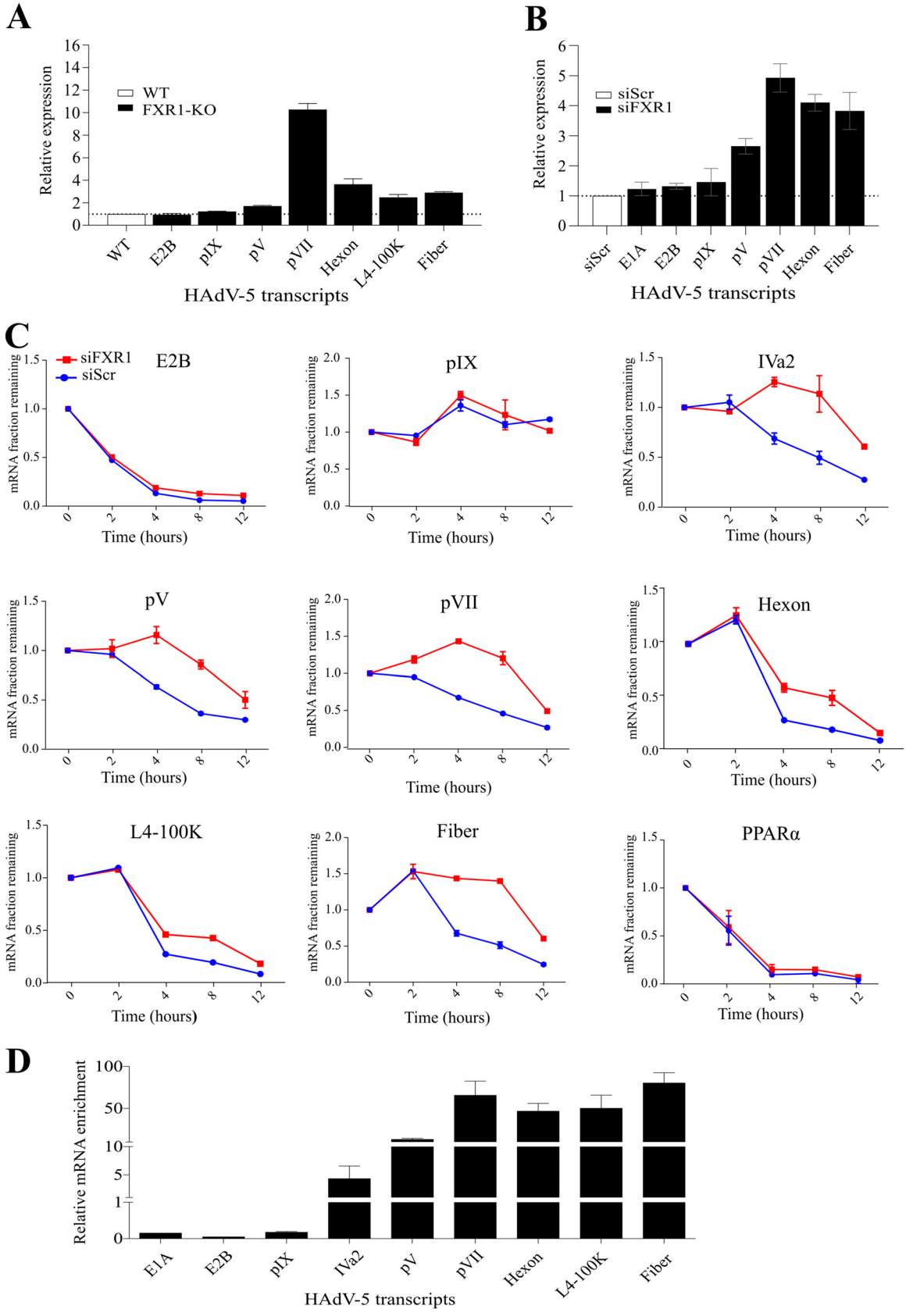

FIG 3 FXR1 deficiency increases the stability of the MLTU mRNAs. (A) Accumulation of HAdV-5 early (E2B), intermediate (pIX), and late (pV, pVII, hexon, L4-100K, fiber) mRNAs in control A549 (WT, expressing Cas9) and CRISPR/Cas9-modified A549 (FXR1-KO) cells. Data

(Continued on next page)

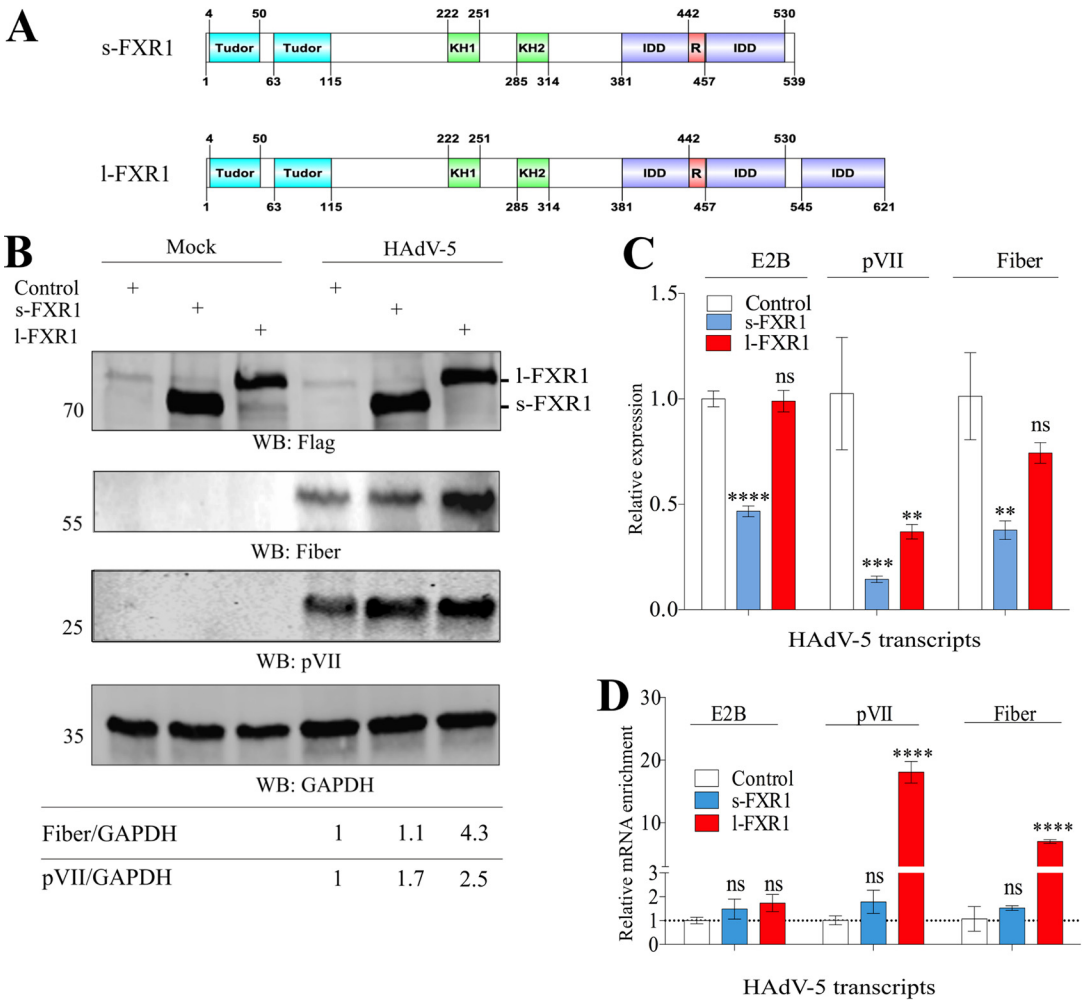

FIG 4 Different roles of the s-FXR1 and l-FXR1 proteins in MLTU mRNA metabolism. (A) A schematic overview of the long FXR1 (l-FXR1) and short FXR1 (s-FXR1) proteins. The indicated Tudor (amino acids [aa] 4 to 50 and aa 6 to 115), KH (aa 222 to 251 and aa 285 to 314), RGG (aa 442 to 457), and IDD (aa 381 to 530 and aa 545 to 621) domains are based on uniprot.org annotation (P51114). (B) Lentivirus-transduced A549 FXR1-KO cells expressing the Flag-s-FXR1 or Flag-l-FXR1 proteins. Cells were infected with HAdV-5 for 24 h, and total cell lysates were analyzed by Western blotting using the anti-Flag, anti-pVII, anti-fiber, and anti-GAPDH antibodies. Control, A549 FXR1-KO transduced with non-FXR1 expressing lentivirus. (C) Virus mRNA (E2B, pVII, fiber) expression in lentivirus-transduced A549 FXR1-KO cells. **, $P < 0.01$; ***, $P < 0.001$; ****, $P < 0.0001$; ns, no significant difference. (D) Binding of the Flag-s-FXR1 or Flag-l-FXR1 proteins to viral mRNA (E2B, pVII, fiber). The CLIP-qPCR data (mean ± SD) are shown as relative mRNA enrichment after considering the anti-Flag immunoprecipitation reaction in the control sample (A549 FXR1-KO transduced with non-FXR1 expressing lentivirus) as 1. ****, $P < 0.0001$; ns, no significant difference.

The l-FXR1 isoform enhances the translation of HAdV-5 tripartite leader element-containing reporter mRNA. One particular feature of the MLTU transcripts is that they contain the tripartite leader (TPL) element as the 5′ untranslated region (UTR) of the mRNA (38). The TPL is a short, structured RNA element generated by constitutive splicing of 3 exons (leader 1, 2, 3) (Fig. 1A) (39). The TPL is needed to translate viral

FIG 3 Legend (Continued)
(mean ± SD) are shown as relative expression of a virus-specific transcript in A549 FXR1-KO cells compared to A549 WT cells after normalization to 18S rRNA. (B) Accumulation of HAdV-5 early (E1A, E2B), intermediate (pIX), and late (pV, pVII, hexon, fiber) mRNAs in the siScr- and siFXR-treated HeLa cells. Data (mean ± SD) are shown as relative expression of a virus-specific transcript in the siFXR-treated sample compared to the siScr-treated sample after normalization to 18S rRNA. (C) FXR1 knock-down increases HAdV-5 MLTU mRNA stability. siRNA-transfected and HAdV-5-infected HeLa cells were treated with actinomycin D (ActD) to block transcription. Cytoplasmic RNA was isolated at the indicated time points after ActD treatment, and mRNA abundance was analyzed with qRT-PCR as in panel B. The relative accumulation of mRNA (mean ± SD) after considering ActD addition time point ($t = 0$) is 1. (D) The endogenous FXR1 protein was immunoprecipitated from HAdV-5-infected HeLa cells, and its bound mRNAs were detected using RT-qPCR (CLIP-qPCR assay). A nonspecific antibody sample (IgG) was used as the immunoprecipitation specificity control. Data (mean ± SD) are shown as a relative enrichment of virus transcripts in the anti-FXR1 antibody sample after normalization to the IgG sample (IgG = 1).

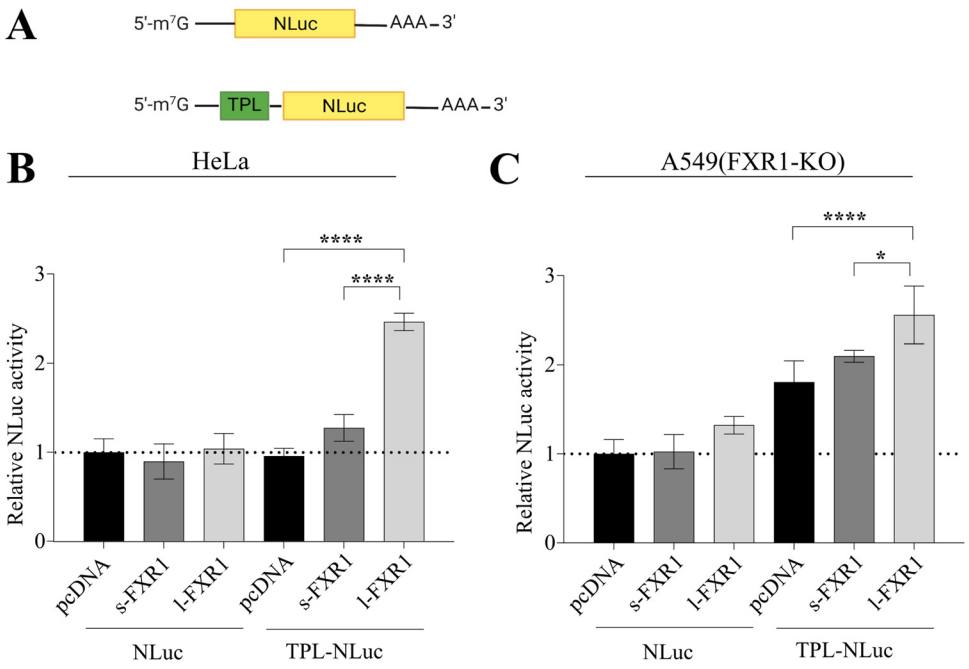

FIG 5 The l-FXR1 protein enhances the translation of HAdV-5 tripartite leader-containing reporter mRNA. (A) Schematic overview of the NanoLuc (NLuc) and tripartite (TPL) element-containing NLuc (TPL-NLuc) mRNAs. (B and C) HeLa cells (B) or A549 FXR1-KO cells (C) were transiently transfected with the respective Flag-tagged FXR1 plasmids for 24 h, followed by NLuc or TPL-NLuc mRNA transfection for 16 h. Quantitative measurement of the NLuc activity was regarded as the mRNA translation read-out. Data are shown as the mean ± SD; relative NLuc activity was calculated after considering pcDNA plus the NLuc sample as 1. *, $P < 0.05$; ****, $P < 0.0001$.

capsid mRNAs during the late phase of the HAdV infection (40, 41). Since the accumulation of the pVII and fiber proteins was reduced in A549 FXR1-KO cells (Fig. 2A), we hypothesized that the FXR1 isoforms might target the TPL element to regulate protein synthesis. To test this hypothesis, a NanoLuc (NLuc) reporter or a TPL-containing NLuc (TPL-NLuc) reporter mRNA (Fig. 5A) was synthesized *in vitro* and transiently transfected along with the s-FXR1- or l-FXR1-expressing plasmids into HeLa or A549 FXR1-KO cells. Translation of the transfected NLuc and TPL-NLuc reporter mRNAs were detected by measuring NLuc enzymatic activity. Expression of the s-FXR1 or l-FXR1 proteins did not significantly change NLuc mRNA translation in HeLa (Fig. 5B) or A549 FXR1-KO (Fig. 5C) cells. In contrast, TPL-NLuc mRNA translation was significantly enhanced in the presence of the l-FXR1 protein in both tested cell lines (Fig. 5B and C).

Together, our data suggest that the l-FXR1 protein can enhance TPL-containing mRNA translation in HeLa and A549 cells.

The s-FXR1 protein forms distinct subcellular condensates in HAdV-5-infected cells. A recent study has shown that mouse FXR1 isoforms exhibit altered subcellular localization depending on the length of their IDD (29). To test the subcellular localization of the human FXR1 isoforms, immunofluorescence experiments were performed both in lentivirus-transduced A549 FXR1-KO and in plasmid-transfected HeLa cells. Wide-field microscopy showed that the Flag-FXR1 isoforms were predominantly localized to the cytoplasm in both cell lines (Fig. 6A). Remarkably, the Flag-s-FXR1 protein formed distinct enlarged cytoplasmic condensates in noninfected and HAdV-5-infected cells (Fig. 6A). A similar staining pattern was not observed in the Flag-l-FXR1-expressing A549 FXR1-KO and HeLa cells. The formation of these condensates in A549 FXR1-KO cells was not due to differences in the FXR1 protein expression, as both isoforms were detected at similar intensities by Western blotting (Fig. 4B). Reanalysis of the same A549 FXR1-KO cell samples (Fig. 6A, left panel) with confocal microscopy confirmed

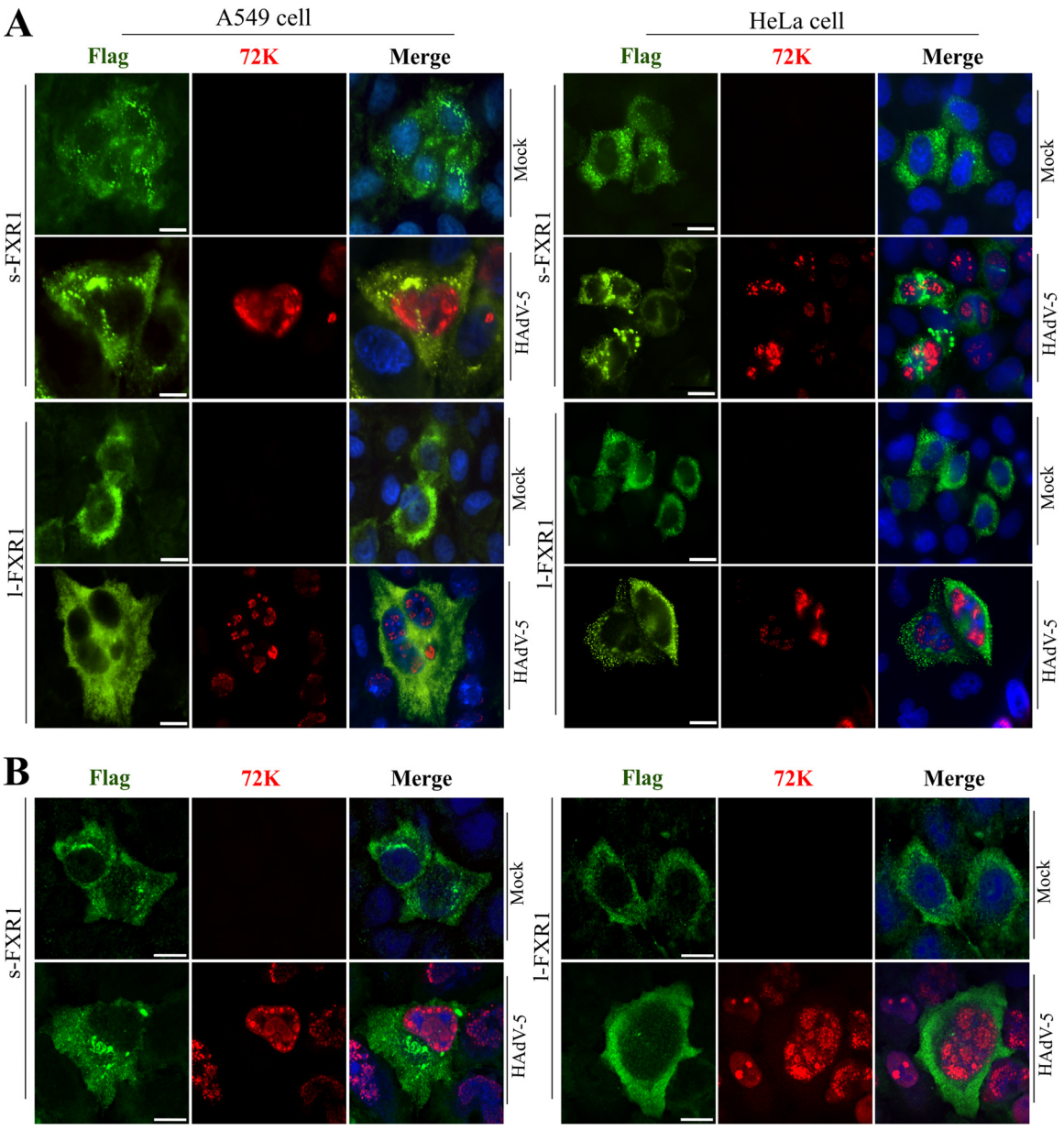

FIG 6 The s-FXR1 protein forms distinct subcellular condensates in HAdV-5-infected cells. (A, left panels) Lentivirus-transduced A549 FXR1-KO cells expressing the Flag-s-FXR1 or Flag-l-FXR1 proteins. (A, right panels) HeLa cells were transiently transfected with the Flag-s-FXR1 or Flag-l-FXR1 protein-expressing plasmids. Both cell lines were infected with HAdV-5 (MOI, 5; 24 hpi). Indirect immunofluorescence was done using the anti-Flag (detects Flag-tagged FXR1) and anti-E2-72K (marker for virus infection) antibodies. Cells were analyzed with a wide-field microscope and counterstained with DAPI. Scale bar = 10 μm. (B) The same A549 FXR1-KO experiment as in panel A, but cells were analyzed with a confocal microscope.

that the s-FXR1 condensates did not overlap the virus nuclear replication centers (72K staining) (Fig. 6B).

Overall, our results suggest that the s-FXR1 and l-FXR1 proteins show different cytoplasmic accumulation patterns in HAdV-infected cells.

Enhanced binding of l-FXR1 to m^{6}A-modified MLTU mRNAs. A recent study has shown that many HAdV-5 MLTU mRNAs are m^{6}A-modified (7). Notably, specific m^{6}A reader proteins recognize the m^{6}A-modified mRNAs (42). The FXR1 protein has been shown to interact with m^{6}A-modified RNAs and has therefore been proposed as a potential novel m^{6}A reader protein (43). To test whether the endogenous FXR1 protein binds to m^{6}A-modified MLTU mRNAs, the CLIP-qPCR was performed (Fig. 7A). As a

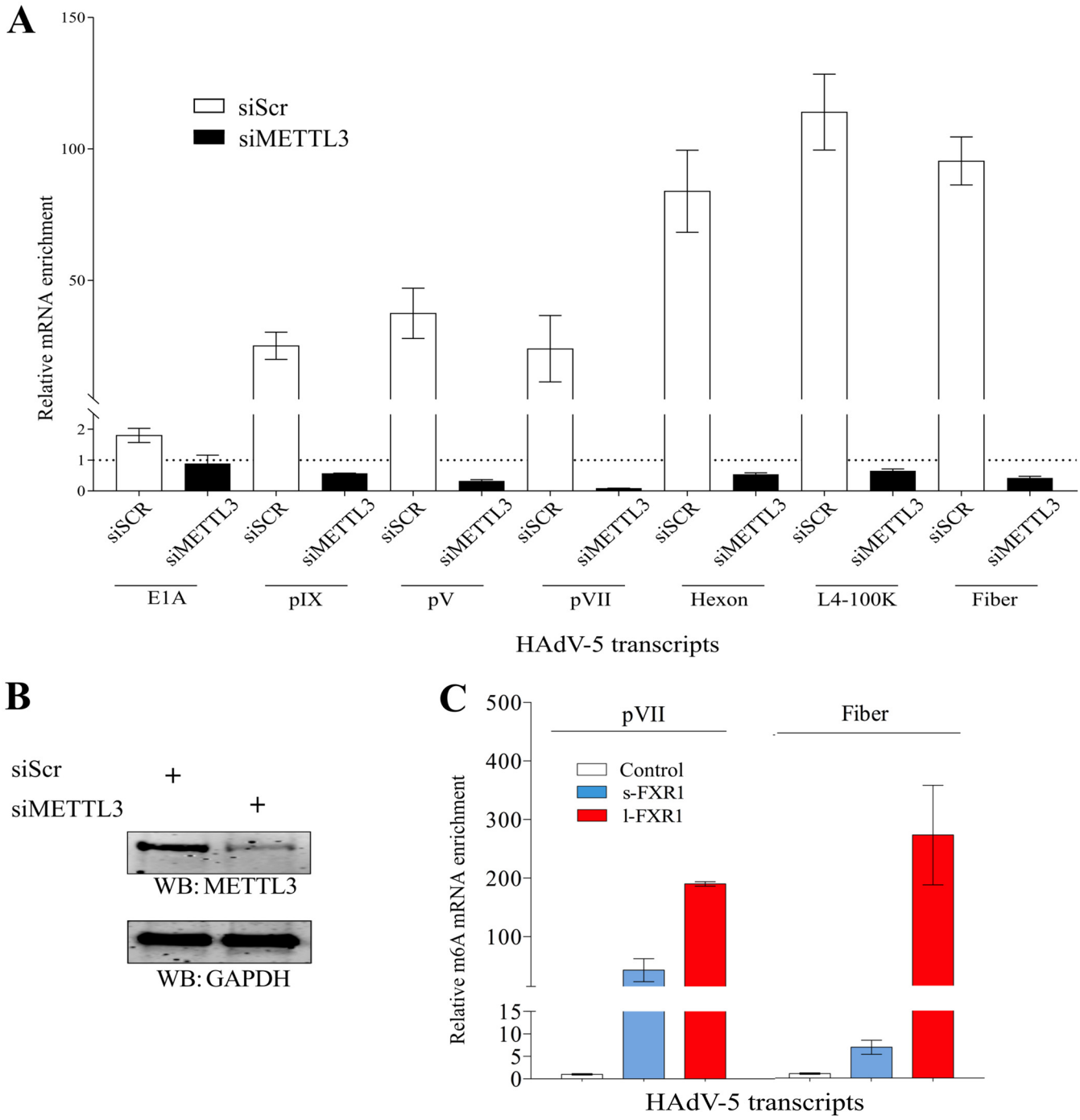

FIG 7 FXR1 binds to m^{6}A-modified HAdV-5 transcripts. (A) Endogenous FXR1 was immunoprecipitated from siScr- or siMETTL3-treated and HAdV-5-infected (48 hpi) A549 cells. CLIP-qPCR results (mean ± SD) are shown as a relative enrichment of specific virus mRNA in the FXR1 antibody sample after normalization to the control IgG sample (IgG = 1). (B) Western blot showing the efficiency of siMETTL3. (C) Lentivirus-transduced A549 FXR1-KO cells expressing the Flag-s-FXR1 or Flag-l-FXR1 proteins were infected with HAdV-5 (MOI, 5; 24 hpi). m^{6}A-containing RNAs were immunopurified from total RNA with an anti-m^{6}A antibody in all three cell samples. RT-qPCR results (mean ± SD) are shown as a relative enrichment of m^{6}A-modified viral transcripts in the Flag-s-FXR1 or Flag-l-FXR1 samples compared to the control sample (control = 1). Control, A549 FXR1-KO transduced with non-FXR1 expressing lentivirus.

specificity control, the m^{6}A modification was eliminated by treating the cells with an siRNA against the m^{6}A writer protein METTL3 (Fig. 7B). The endogenous FXR1 protein binding to different viral mRNAs was lost in the absence of the m^{6}A modification (Fig. 7A). The m^{6}A modification is a dynamic process controlled by an interplay between different m^{6}A writer, reader, and eraser proteins (42). Considering FXR1 as an m^{6}A reader protein, we tested whether individual FXR1 isoforms influence the m^{6}A

modification on HAdV-5 mRNAs. To this end, we used an anti-m^{6}A antibody to immunopurify viral m^{6}A-containing mRNAs from the lentivirus-transduced A549 FXR1-KO cells. Expression of the Flag-s-FXR1 or Flag-l-FXR1 proteins increased the m^{6}A signal in the pVII and fiber transcripts (Fig. 7C). Noticeably, the l-FXR1 protein expression correlated with a more drastic increase of the m^{6}A signal compared to the s-FXR1 protein expression.

Overall, our results suggest that the m^{6}A modification is needed for FXR1 binding to the MLTU mRNAs and that expression of the FXR1 isoforms protects m^{6}A modification in the pVII and fiber transcripts.

DISCUSSION

FXR1 is an RNA-binding protein that regulates mRNA localization, stability, and translation (22–25, 27, 44). Moreover, FXR1 controls muscle and neuron development and has a potential oncogenic role in many cancers (17, 29, 45). Despite a detailed knowledge of the role of FXR1 in cellular gene expression, very little is known about its exact functions in virus infections (46, 47). Notably, more is known about the functions of the FXR1 homolog FMRP1 protein in virus-infected cells. For example, the FMRP1 protein has been described as a Zika virus (ZIKV) restriction factor since it interacts with and blocks the ZIKV RNA translation (48). Here, we investigated the role of FXR1 during lytic HAdV-5 infection. We show that the FXR1 protein can bind to the MLTU mRNAs (Fig. 3D and 4D) and reduce their stability (Fig. 3C) and that it is needed for the formation of infectious progeny (Fig. 2C). In addition, we show that the l-FXR1 isoform is specifically targeting MLTU mRNA (pVII, fiber) and the TPL element, hence suggesting its dedicated involvement in HAdV-5 capsid mRNA translation.

HAdV MLTU mRNAs accumulate in massive amounts during the late phase of infection because virus DNA replication produces hundreds of thousands of new templates for the transcription (49). However, our data indicate that the MLTU mRNA levels are also controlled by the FXR1 protein-mediated mRNA degradation. First, the steady-state levels of virus late (i.e., MLTU), but not early/intermediate, mRNAs were higher in the FXR1 knockout and knockdown cells (Fig. 3A and 3B). Second, several MLTU mRNAs showed extended stability in the FXR1-deficient cells (Fig. 3C). Notably, the decay of the pV, pVII, and fiber mRNAs correlated with the FXR1 protein binding to these viral mRNAs (Fig. 3D). Although the endogenous FXR1 protein interacted with all tested viral MLTU mRNAs (pV, pVII, hexon, L4-100K, fiber), only three of them (pV, pVII, fiber) showed remarkably different stability in the FXR1-deficient cells (Fig. 3C). This may indicate that additional cellular or viral proteins are involved in FXR1-dependent MLTU mRNA turnover. In line with our study, Herman et al. demonstrated that FXR1 binds to several inflammatory mRNAs and decreases their stability (27). Mechanistically, counteracting interactions between the RNA-destabilizing FXR1 and RNA-stabilizing HuR proteins on AU-rich element (ARE)-containing transcripts were suggested to cause the mRNA decay. A previous study showed that the HuR protein stabilizes canonical ARE-containing reporter gene transcripts in HAdV-infected cells (50). The HuR protein can also stabilize HAdV IVa2 mRNA, as it contains a canonical ARE (50). Therefore, we considered a potential FXR1-HuR interaction on ARE-containing transcripts as a mechanism for MLTU mRNA turnover. This hypothesis was supported by our ActD-treatment experiment, which showed that the HuR-regulated, ARE-containing IVa2 transcript was indeed more stable in the FXR1 knockdown cells (Fig. 3C). The observation that endogenous FXR1 interacted with the IVa2 mRNA (Fig. 3D) further supported the hypothesis that FXR1 might target ARE-containing mRNAs in HAdV-5-infected cells. However, our bioinformatics analysis did not identify any canonical or noncanonical AREs in the MLTU mRNAs. Based on our study and the report by Jehung et al. (50), it is possible that FXR1 targets IVa2 mRNA in an ARE-dependent manner, whereas the MLTU mRNAs are targeted in an ARE-independent manner. Although most of the MLTU transcripts contain TPL, there are additional sequence elements that may control MLTU mRNA stability, for example, the noncoding linker sequence between TPL and the first AUG of the respective MLTU mRNA, the coding sequence of particular MLTU mRNA, and the 3′ end of the MLTU mRNA. It is possible that

these sequence elements are targeted by the FXR1 protein. Overall, the exact mechanism(s) of how the FXR1 protein targets defined MLTU mRNAs for degradation remains elusive.

Recent studies have shown that FXR1 is a novel m^{6}A reader protein (43, 46). Notably, Price and colleagues (7) demonstrated that elimination of the m^{6}A catalyzing enzyme METTL3 drastically reduced capsid protein accumulation and significantly lowered infectious HAdV-5 progeny due to reduced splicing of MLTU pre-mRNAs. Surprisingly, the elimination of the cytoplasmic m^{6}A readers YTHDF1, YTHDF2, and YTHDF3 had a minimal effect on the HAdV-5 infectious cycle in their study (7). These observations may suggest that another cytoplasmic m^{6}A reader protein, such as FXR1, targets m^{6}A-modified MLTU mRNAs and controls their stability and translation. Indeed, endogenous FXR1 specifically binds to m^{6}A-modified MLTU transcripts (Fig. 7A), and both s-FXR1 and l-FXR1 protect m^{6}A signal on the pVII and fiber mRNAs (Fig. 7C). Notably, the l-FXR1 protein had a more dominant effect on the fiber protein (Fig. 4B) and on m^{6}A-modified fiber mRNA (Fig. 7C) compared to s-FXR1. This might indicate that l-FXR1 regulates fiber mRNA translation, particularly in an m^{6}A-dependent manner.

Our study is the first to shed light on two human FXR1 isoforms, s-FXR1 and l-FXR1, in virus-infected cells. Most human FXR1 studies have been carried out using s-FXR1, leaving l-FXR1 functions relatively unexplored. Since both isoforms contain the same Tudor, KH, and RGG domains (Fig. 4A), it is intuitive to think that both isoforms bind equally well to mRNA. However, based on our experiments, only the l-FXR1 protein, and not s-FXR1, interacted with the pVII and fiber mRNAs in A549 cells. Furthermore, l-FXR1 MLTU mRNA binding correlated with the increased translation of the TPL-containing reporter mRNA (Fig. 5). These observations may suggest that l-FXR1 binding to TPL enhances viral capsid mRNA translation. Since the s-FXR1 and l-FXR1 differ in the length of their C-terminal IDD (Fig. 4A), we speculate that the posttranslational modifications within the IDD domain permit l-FXR1 to bind better to MLTU mRNAs than s-FXR1. Indeed, the extended IDD in l-FXR1 is serine/threonine- and lysine rich, which theoretically supports its posttranslational modification by phosphorylation and acetylation, respectively. In contrast to l-FXR1, expression of the s-FXR1 protein induced the formation of the enigmatic biomolecular condensates (Fig. 6). A recent study has shown that the longest mouse FXR1 protein, known as isoform E, can promote the formation of biomolecular condensates, similar to what we see in our study (Fig. 6) (29). Since the function of these FXR1 condensates remains unclear, further studies are warranted to understand the exact constituents and role of these condensates in both non- and virus-infected cells.

Surprisingly, MLTU mRNA and protein expression in FXR1-depleted cells did not correlate: tested MLTU mRNAs (i.e., pVII, fiber) showed enhanced accumulation, whereas the respective protein levels were reduced (Fig. 2A, 3A, and 3B). We speculate that this might be due to opposing functions of the s-FXR1 and l-FXR1 proteins in infected cells. We envision that the multifunctional l-FXR1 protein can bind to and enhance translation of the TPL-containing (i.e., MLTU) mRNAs during infection. In contrast, the s-FXR1 protein is more efficient than l-FXR1 in reducing the viral mRNAs' stability. Accordingly, the elimination of both isoforms, by either siRNA or CRISPR/Cas9, will generate a situation whereby MLTU mRNAs are stabilized due to the lack of the s-FXR1 protein. At the same time, the pVII and fiber mRNAs will not be translated due to the lack of the l-FXR1 protein. Hence, the proper balance between the l-FXR1 and s-FXR1 proteins or possibly even between the different members of the FXR protein family (FXR1, FXR2, FMR1) may fine-tune MLTU metabolism in infected cells.

The majority of HAdV-5 infections cause self-limiting diseases. However, life-threatening HAdV-5 infections occur, particularly among solid organ transplant recipients (51). Based on our study, the l-FXR1 protein acts as the cellular proviral factor enhancing the translation of viral capsid proteins. Therefore, specific targeting and elimination of the l-FXR1 protein might be considered as a potential therapeutic option to treat life-threatening HAdV-5 infections.

Taken together, our study identifies FXR1, and particularly l-FXR1, as a novel regulator of the MLTU mRNA metabolism during the lytic HAdV-5 life cycle.

MATERIALS AND METHODS

Cell lines. The HeLa and A549 cells were obtained from ATCC. The cell lines were grown in Dulbecco's modified Eagle medium (DMEM; Invitrogen) supplemented with 10% fetal bovine serum (FBS) and penicillin-streptomycin solution (PEST; Gibco) at 37°C in a 5% CO_2 incubator. CRISPR/Cas9 genome editing was used to generate the FXR1 protein-deficient A549 cell line (FXR1-KO). The guide RNA (5′-CAAATGACCAAGAGCCATGT-3′) was designed and cloned into the pSpCas9 (BB)-2A-Puro (PX459) V.2.0 (Addgene no. 62988) plasmid as described previously (52). Individual clones were isolated using puromycin selection (1 μg/mL final concentration [conc.]). The control A549 cell line (WT) was transfected with the pSpCas9 (BB)-2A-Puro (PX459) V.2.0 plasmid, which expresses the Cas9 protein but lacks the specific guide RNA sequence.

Plasmids, siRNA, and bioinformatics analysis. Plasmid expressing s-FXR as an N-terminal Flag-tagged protein was generated by recloning the s-FXR cDNA from plasmid pFRT-TODestFLAGHAhFXR1 (Addgene plasmid no. 48694) into the pcDNA3-N-Flag background (pcDNA-Flag-s-FXR1). Plasmid expressing l-FXR1 was generated by inserting l-FXR1 gBlock (IDT) sequence into PflMI (cleaves within FXR1 cDNA) and XhoI (cleaves within pcDNA3 vector) sites in the pcDNA-Flag-s-FXR1. HAdV-5 tripartite leader (TPL) element (203 bp, gBlock [IDT]) was inserted into the HindIII site in NanoLuc-expressing pNL1.1.PGK (Promega) plasmid. Bioinformatics analysis regarding the ARE sequences in the HAdV-5 genome (AC_000008.1) was performed using CLC Main Workbench (Qiagen). siScr (5′-AGGUAGUGUAAU CGCCUUG-3′), siFXR1 (5′-CGAGCUGAGUGAUUGGUCAdTdT-3′), and siMETTL3 (5′-CUGCAAGUAUGUUCA CUAUGAdTdT-3′) were purchased from Eurofins Genomics.

Transfection. Plasmid transfections were performed with JetPrime (Polyplus) transfection reagent according to the manufacturer's protocol. Similarly, the siRNA transfections were done using JetPrime reagent at a final concentration of 45 nM. For mRNA transfections jetMESSENGER reagent (Polyplus) was used (see below).

Virus infection. Virus infections and titrations were carried out using replication-competent HAdV-5 as described previously (53). All of the HAdV-5 infections were performed at a multiplicity of infection (MOI) of 5, defined as fluorescence-forming units (FFU/cell), in infection medium (DMEM plus 2% newborn calf serum [NCS] without any supplements). After 1 h of incubation at 37°C in a 5% CO_2 incubator, virus-containing infection medium was replaced with the normal growth medium (DMEM containing FBS and PEST).

Lentiviruses. Flag-s-FXR1 and Flag-l-FXR1 sequences were cloned into pLVX-EF1alpha-eGFP-2xStrep-IRES-Puro transfer plasmid (Addgene no. 141395) using EcoRI and BamHI restriction enzymes. The control transfer plasmid (pLenti_empty, does not express FXR1) was made by refilling BamHI and EcoRI cohesive ends with the Klenow enzyme. Lentiviruses were produced by transfection of the respective transfer plasmid along with the envelope (pMD2.G, Addgene no. 12259) and packaging plasmids (psPAX2, Addgene no. 12260) into Lenti-X 293T cells (TaKaRa). Cell supernatants were collected, filtrated, and used to infect A549 FXR1-KO cells. Cells were selected with puromycine (1 μg/mL) for 4 days; after that, the surviving cells were expanded.

Primary antibodies and reagents. The following antibodies were used for Western blotting experiments: anti-rabbit HAdV capsid (Abcam, ab6982), anti-mouse Flag (Sigma, M2, F1804), anti-mouse pVII (no. 2-14 [54]), anti-mouse fiber (Invitrogen, 4D2), anti-mouse FXR1 (Millipore, no. 05-1529), anti-mouse GAPDH (Santa Cruz, sc-365062), anti-rabbit METTL3 (Abcam, ab240595), anti-goat actin (Santa Cruz). The following antibodies were used for immunofluorescence experiments: anti-rabbit E2A-72K (kindly provided by Bruce Stillman; 1:1,000), anti-mouse Flag (Sigma, M2, F1804; 1:1,000). Actinomycin D was purchased from Sigma (A1410) and was dissolved in dimethyl sulfoxide (DMSO).

Infectious virus determination. HeLa cells were transfected with siScr or siFXR1 for 48 h, followed by infection with the Ad5-Luc3 virus (MOI, 5) (36). Both cell growth medium (extracellular virus) and cell pellets (intracellular virus) were collected at 24 hpi and stored at −80°C. The cell pellet was resuspended in 100 μL of 0.1 M Tris-HCl (pH 8.0), freeze-thawed three times, and centrifuged to separate cell supernatant and cell debris. The same volume of the cell supernatant and the cell growth medium were used to reinfect fresh HeLa cells in a 24-well plate for 1 h. Cells were lysed 24 hpi in passive lysis buffer (Promega), and firefly luciferase reporter gene expression was detected using the Luciferase reporter assay system (Promega) and analyzed on a TECAN Infinite M200 plate reader.

Western blotting. The whole-cell lysates were prepared as described previously (35). The proteins were separated on AnyKD (Bio-Rad) SDS-PAGE, transferred to a nitrocellulose membrane, and incubated with primary antibody at 4°C overnight. Proteins were detected by fluorescence-labeled secondary antibody IRDye 680 or IRDye 800 (LI-COR) and visualized with an Odyssey CLX imaging system (LI-COR).

Immunofluorescence assays. Cells were grown on coverslips, transfected with plasmid DNA (HeLa cells only), and infected with HAdV-5 (MOI of 5, 24 hpi). Lentivirus-transduced A549 FXR1-KO cells were infected with HAdV-5 (MOI of 5, 24 hpi). Cells were fixed in 4% paraformaldehyde for 10 min, followed by cell permeabilization with 0.1% Triton X-100 in PBST (phosphate-buffered saline [PBS] plus 0.01% Tween20) for 10 min at room temperature. After blocking the cells with 2% bovine serum albumin (BSA)/PBST solution for 1 h, the coverslips were incubated with the primary antibodies diluted in blocking solution overnight at 4°C. Proteins were visualized with the fluorescein isothiocyanate (FITC)- and tetramethyl rhodamine isocyanate (TRITC)-conjugated secondary antibodies (Sigma, F6005 and T5393)

for 1 h at room temperature. Nuclei were stained with DAPI (4′,6-diamidino-2-phenylindole) supplemented in the Fluoromount-G mounting medium (Thermo Fisher). Slides were analyzed with a widefield fluorescence microscope (Nikon Eclipse 90i), and the images were analyzed with NIS-Elements (Nikon) software. Some slides were analyzed with a confocal microscope (Zeiss LSM700) and analyzed with Fiji software.

RNA isolation and qRT-PCR. Total RNA was isolated using TRIreagent (Sigma), and contaminating genomic DNA was removed using a RapidOut DNA removal kit (Thermo Scientific). About 500 ng of RNA was used for cDNA synthesis using SuperScript III reverse transcriptase (Invitrogen) and random primers. Quantitative reverse transcription-PCR (qRT-PCR) reactions were performed using HOT FIREPoL EvaGreen supermix (Solis BioDyne) in a QuantStudio 6 Flex real-time PCR system (Applied Biosystems). Every sample was run in triplicate and normalized against the expression of housekeeping genes (GAPDH [glyceraldehyde-3-phosphate dehydrogenase] or 18S rRNA). Sequences of the used viral and cellular primers are available in Table S1 in the supplemental material.

mRNA transfection. To generate NLuc and TPL-NLuc mRNAs, the respective reporter gene sequence was PCR amplified from pNL1.1.PGK and pNL1.1-Trip.PGK plasmids using T7 promoter containing primers T7-NLuc and T7-TPL-NLuc (Table S1). Purified T7-containing PCR products were used as the templates for *in vitro* transcription with the HiScribe T7 ARCA mRNA kit (with tailing; NEB) according to the manufacturer's protocol. Synthesized reporter mRNAs were purified using an RNA cleanup and concentrator kit (Zymo), and the integrity and polyadenylation of the mRNAs were verified by agarose gel electrophoresis. Semiconfluent HeLa or A549 FXR1-KO cells on a 24-well plate were first transfected with 1 μg of the respective Flag-FXR1 plasmid using JetPrime reagent. Then, 24 h after plasmid DNA transfection, the cells were transfected with 1 ng of either NLuc or TPL-NLuc mRNA using jetMESSENGER reagent (Polyplus). Cells were lysed in passive lysis buffer (Promega) 16 h after mRNA transfection. NLuc activity was measured in quadruplets with a TECAN Infinite M200 plate reader using the Nano-Glo luciferase assay system (Promega).

Actinomycin D treatment. HeLa cells were transfected with siScr or siFXR1 for 48 h, followed by HAdV-5 infection (MOI, 5) for an additional 24 h. Actinomycin D (ActD) was diluted to a final concentration of 5 μg/mL in cell growth medium and was added to the cells (t = 0). Total RNA was isolated from the cells at defined time points (t = 2 h, 4 h, 8 h, 12 h) after ActD treatment. RNA extraction, cDNA synthesis, and mRNA expression were carried out as described above.

RNA cross-linking immunoprecipitations followed by RT-qPCR (CLIP-qPCR). The CLIP-qPCR experiments were done as described previously (32) with minor modifications. Cells were washed once with ice-cold 1× phosphate-buffered saline (PBS) and irradiated three times with 400 mJ/cm^2 (254 nm) in a CL-1000 UV crosslinker (UVP). Cells were lysed in buffer 3 (50 mM HEPES-KOH, pH 7.9, 150 mM NaCl, 0.5% Na-deoxycholate, 0.1% SDS) supplemented with Halt proteases (Thermo Scientific). The anti-FLAG M2 affinity beads (A2220, Sigma) were used to immunopurify Flag-tagged FXR1 proteins by incubating cell lysates with the beads overnight at 4°C. The beads were washed twice with high-salt wash buffer (50 mM HEPES-KOH, pH 7.9, 1 M NaCl, 0.5% Na-deoxycholate, 0.1% SDS) and twice with low-salt wash buffer (50 mM HEPES-KOH, pH 7.9, 10 mM NaCl, 0.5% Na-deoxycholate, 0.1% SDS). Afterward, the beads were incubated with DNase I for 30 min at 37°C, followed by proteinase K (40 μg) digestion in buffer K (125 mM Tris-HCl, pH 7.8, 62.5 mM NaCl, 12.5 mM EDTA) for 1 h at 56°C. RNA isolation, cDNA synthesis, and RT-qPCR were carried out as described above. CLIP-qPCR with the endogenous FXR1 was performed using rabbit IgG antibody (Cell Signaling Technologies, no. 2729S) and anti-FXR1 antibody (Millipore, no. 05-1529). The immunocomplexes were collected with protein G Sepharose beads (GE Healthcare) for 2 h on a rotating wheel at 4°C. Primer sequences are shown in Table S1.

m^{6}A RNA immunoprecipitation. Lentivirus-transduced A549 FXR1-KO cell lines (control [non-FXR1 expressing], Flag-s-FXR1, Flag-l-FXR1) were infected with HAdV-5 (MOI of 5, 24 hpi). Total RNA was extracted with TRIreagent, and contaminating genomic DNA was removed with a RapidOut DNA removal kit (Thermo Scientific). About 4 μg of an anti-m^{6}A antibody (SySy, no. 202011) or normal rabbit IgG antibody was added to 20 μg of total RNA in immunoprecipitation (IP) buffer (50 mM Tris pH 7.4, 100 mM NaCl, 0.05% NP40), and samples were incubated overnight at 4°C. The next day, protein G Sepharose beads were added to the samples and incubated for 2 h on a rotating wheel at 4°C. The beads were washed twice with high-salt buffer (50 mM Tris, pH 7.4, 1 M NaCl, 1 mM EDTA, 1% NP40, 0.1% SDS) and 4 times with IP buffer. RNA purification, cDNA synthesis, and RT-qPCR were performed as described above. The primers used are shown in Table S1.

Statistical analysis. Data were analyzed with Prism 6.0c software (GraphPad Software, Inc.). Results are expressed as the mean (n = 3) with standard deviation (SD). The nonparametric Kruskal-Wallis test or independent-sample t test was used for statistical analysis.

SUPPLEMENTAL MATERIAL

Supplemental material is available online only.

SUPPLEMENTAL FILE 1, PDF file, 0.1 MB.

ACKNOWLEDGMENTS

We thank Wael Kamel for the help with the CLIP-qPCR protocol, Harald Wodrich for the anti-pVII antibody, Raviteja Inturi for CRISPR/Cas9 design and lentivirus purification, Anette Carlsson for excellent technical support, and the rest of our lab members for valuable discussions.

REFERENCES

1. Assadian F, Sandstrom K, Bondeson K, Laurell G, Lidian A, Svensson C, Akusjarvi G, Bergqvist A, Punga T. 2016. Distribution and molecular characterization of human adenovirus and Epstein-Barr virus infections in tonsillar lymphocytes isolated from patients diagnosed with tonsillar diseases. PLoS One 11:e0154814. https://doi.org/10.1371/journal.pone.0154814.
2. Lion T. 2014. Adenovirus infections in immunocompetent and immunocompromised patients. Clin Microbiol Rev 27:441–462. https://doi.org/10.1128/CMR.00116-13.
3. Georgi F, Greber UF. 2020. The adenovirus death protein: a small membrane protein controls cell lysis and disease. FEBS Lett 594:1861–1878. https://doi.org/10.1002/1873-3468.13848.
4. Ip WH, Dobner T. 2020. Cell transformation by the adenovirus oncogenes E1 and E4. FEBS Lett 594:1848–1860. https://doi.org/10.1002/1873-3468.13717.
5. Charman M, Herrmann C, Weitzman MD. 2019. Viral and cellular interactions during adenovirus DNA replication. FEBS Lett 593:3531–3550. https://doi.org/10.1002/1873-3468.13695.
6. Donovan-Banfield I, Turnell AS, Hiscox JA, Leppard KN, Matthews DA. 2020. Deep splicing plasticity of the human adenovirus type 5 transcriptome drives virus evolution. Commun Biol 3:124. https://doi.org/10.1038/s42003-020-0849-9.
7. Price AM, Hayer KE, McIntyre ABR, Gokhale NS, Abebe JS, Della Fera AN, Mason CE, Horner SM, Wilson AC, Depledge DP, Weitzman MD. 2020. Direct RNA sequencing reveals m(6)A modifications on adenovirus RNA are necessary for efficient splicing. Nat Commun 11:6016. https://doi.org/10.1038/s41467-020-19787-6.
8. Westergren Jakobsson A, Segerman B, Wallerman O, Lind SB, Zhao H, Rubin CJ, Pettersson U, Akusjärvi G. 2021. The human adenovirus 2 transcriptome: an amazing complexity of alternatively spliced mRNAs. J Virol 95:e01869-20. https://doi.org/10.1128/JVI.01869-20.
9. Kulanayake S, Tikoo SK. 2021. Adenovirus core proteins: structure and function. Viruses 13:388. https://doi.org/10.3390/v13030388.
10. Kanopka A, Muhlemann O, Akusjärvi G. 1996. Inhibition by SR proteins of splicing of a regulated adenovirus pre-mRNA. Nature 381:535–538. https://doi.org/10.1038/381535a0.
11. Kanopka A, Muhlemann O, Petersen-Mahrt S, Estmer C, Ohrmalm C, Akusjärvi G. 1998. Regulation of adenovirus alternative RNA splicing by dephosphorylation of SR proteins. Nature 393:185–187. https://doi.org/10.1038/30277.
12. Ohrmalm C, Akusjärvi G. 2006. Cellular splicing and transcription regulatory protein p32 represses adenovirus major late transcription and causes hyperphosphorylation of RNA polymerase II. J Virol 80:5010–5020. https://doi.org/10.1128/JVI.80.10.5010-5020.2006.
13. Petersen-Mahrt SK, Estmer C, Ohrmalm C, Matthews DA, Russell WC, Akusjärvi G. 1999. The splicing factor-associated protein, p32, regulates RNA splicing by inhibiting ASF/SF2 RNA binding and phosphorylation. EMBO J 18:1014–1024. https://doi.org/10.1093/emboj/18.4.1014.
14. Törmäanen H, Backström E, Carlsson A, Akusjärvi G. 2006. L4-33K, an adenovirus-encoded alternative RNA splicing factor. J Biol Chem 281:36510–36517. https://doi.org/10.1074/jbc.M607601200.
15. Estmer Nilsson C, Petersen-Mahrt S, Durot C, Shtrichman R, Krainer AR, Kleinberger T, Akusjärvi G. 2001. The adenovirus E4-ORF4 splicing enhancer protein interacts with a subset of phosphorylated SR proteins. EMBO J 20:864–871. https://doi.org/10.1093/emboj/20.4.864.
16. Herrmann C, Dybas JM, Liddle JC, Price AM, Hayer KE, Lauman R, Purman CE, Charman M, Kim ET, Garcia BA, Weitzman MD. 2020. Adenovirus-mediated ubiquitination alters protein-RNA binding and aids viral RNA processing. Nat Microbiol 5:1217–1231. https://doi.org/10.1038/s41564-020-0750-9.
17. Majumder M, Johnson RH, Palanisamy V. 2020. Fragile X-related protein family: a double-edged sword in neurodevelopmental disorders and cancer. Crit Rev Biochem Mol Biol 55:409–424. https://doi.org/10.1080/10409238.2020.1810621.
18. Siomi MC, Siomi H, Sauer WH, Srinivasan S, Nussbaum RL, Dreyfuss G. 1995. FXR1, an autosomal homolog of the fragile X mental retardation gene. EMBO J 14:2401–2408. https://doi.org/10.1002/j.1460-2075.1995.tb07237.x.
19. Kirkpatrick LL, McIlwain KA, Nelson DL. 2001. Comparative genomic sequence analysis of the FXR gene family: FMR1, FXR1, and FXR2. Genomics 78:169–177. https://doi.org/10.1006/geno.2001.6667.
20. Darnell JC, Fraser CE, Mostovetsky O, Darnell RB. 2009. Discrimination of common and unique RNA-binding activities among Fragile X mental retardation protein paralogs. Hum Mol Genet 18:3164–3177. https://doi.org/10.1093/hmg/ddp255.
21. Adams-Cioaba MA, Guo Y, Bian C, Amaya MF, Lam R, Wasney GA, Vedadi M, Xu C, Min J. 2010. Structural studies of the tandem Tudor domains of fragile X mental retardation related proteins FXR1 and FXR2. PLoS One 5:e13559. https://doi.org/10.1371/journal.pone.0013559.
22. Ascano M Jr, Mukherjee N, Bandaru P, Miller JB, Nusbaum JD, Corcoran DL, Langlois C, Munschauer M, Dewell S, Hafner M, Williams Z, Ohler U, Tuschl T. 2012. FMRP targets distinct mRNA sequence elements to regulate protein expression. Nature 492:382–386. https://doi.org/10.1038/nature11737.
23. Bukhari SIA, Truesdell SS, Lee S, Kollu S, Classon A, Boukhali M, Jain E, Mortensen RD, Yanagiya A, Sadreyev RI, Haas W, Vasudevan S. 2016. A specialized mechanism of translation mediated by FXR1a-associated MicroRNP in cellular quiescence. Mol Cell 61:760–773. https://doi.org/10.1016/j.molcel.2016.02.013.
24. Vasudevan S, Steitz JA. 2007. AU-rich-element-mediated upregulation of translation by FXR1 and Argonaute 2. Cell 128:1105–1118. https://doi.org/10.1016/j.cell.2007.01.038.
25. Estes PS, O'Shea M, Clasen S, Zarnescu DC. 2008. Fragile X protein controls the efficacy of mRNA transport in Drosophila neurons. Mol Cell Neurosci 39:170–179. https://doi.org/10.1016/j.mcn.2008.06.012.
26. Fan Y, Yue J, Xiao M, Han-Zhang H, Wang YV, Ma C, Deng Z, Li Y, Yu Y, Wang X, Niu S, Hua Y, Weng Z, Atadja P, Li E, Xiang B. 2017. FXR1 regulates transcription and is required for growth of human cancer cells with TP53/FXR2 homozygous deletion. Elife 6:e26129. https://doi.org/10.7554/eLife.26129.
27. Herman AB, Vrakas CN, Ray M, Kelemen SE, Sweredoski MJ, Moradian A, Haines DS, Autieri MV. 2018. FXR1 is an IL-19-responsive RNA-binding protein that destabilizes pro-inflammatory transcripts in vascular smooth muscle cells. Cell Rep 24:1176–1189. https://doi.org/10.1016/j.celrep.2018.07.002.
28. Le Tonqueze O, Kollu S, Lee S, Al-Salah M, Truesdell SS, Vasudevan S. 2016. Regulation of monocyte induced cell migration by the RNA binding protein, FXR1. Cell Cycle 15:1874–1882. https://doi.org/10.1080/15384101.2016.1189040.
29. Smith JA, Curry EG, Blue RE, Roden C, Dundon SER, Rodriguez-Vargas A, Jordan DC, Chen X, Lyons SM, Crutchley J, Anderson P, Horb ME, Gladfelter AS, Giudice J. 2020. FXR1 splicing is important for muscle development and biomolecular condensates in muscle cells. J Cell Biol 219:e201911129. https://doi.org/10.1083/jcb.201911129.
30. Zhao H, Chen M, Lind SB, Pettersson U. 2016. Distinct temporal changes in host cell lncRNA expression during the course of an adenovirus infection. Virology 492:242–250. https://doi.org/10.1016/j.virol.2016.02.017.
31. Zhao H, Konzer A, Mi J, Chen M, Pettersson U, Lind SB. 2017. Posttranscriptional regulation in adenovirus infected cells. J Proteome Res 16:872–888. https://doi.org/10.1021/acs.jproteome.6b00834.
32. Younis S, Kamel W, Falkeborn T, Wang H, Yu D, Daniels R, Essand M, Hinkula J, Akusjarvi G, Andersson L. 2018. Multiple nuclear-replicating viruses require the stress-induced protein ZC3H11A for efficient growth. Proc Natl Acad Sci U S A 115:E3808–E3816.
33. Chroboczek J, Bieber F, Jacrot B. 1992. The sequence of the genome of adenovirus type 5 and its comparison with the genome of adenovirus type 2. Virology 186:280–285. https://doi.org/10.1016/0042-6822(92)90082-z.
34. Inturi R, Mun K, Singethan K, Schreiner S, Punga T. 2018. Human adenovirus infection causes cellular E3 ubiquitin ligase MKRN1 degradation involving the viral core protein pVII. J Virol 92:e01154-17. https://doi.org/10.1128/JVI.01154-17.
35. Mun K, Punga T. 2019. Cellular zinc finger protein 622 hinders human adenovirus lytic growth and limits binding of the viral pVII protein to virus DNA. J Virol 93:e01628-18. https://doi.org/10.1128/JVI.01628-18.
36. Mittal SK, McDermott MR, Johnson DC, Prevec L, Graham FL. 1993. Monitoring foreign gene expression by a human adenovirus-based vector using the firefly luciferase gene as a reporter. Virus Res 28:67–90. https://doi.org/10.1016/0168-1702(93)90090-a.
37. Khandjian EW, Bardoni B, Corbin F, Sittler A, Giroux S, Heitz D, Tremblay S, Pinset C, Montarras D, Rousseau F, Mandel J. 1998. Novel isoforms of the

fragile X related protein FXR1P are expressed during myogenesis. Hum Mol Genet 7:2121–2128. https://doi.org/10.1093/hmg/7.13.2121.
38. Ramke M, Lee JY, Dyer DW, Seto D, Rajaiya J, Chodosh J. 2017. The 5′ UTR in human adenoviruses: leader diversity in late gene expression. Sci Rep 7:618. https://doi.org/10.1038/s41598-017-00747-y.
39. Chow LT, Broker TR. 1978. The spliced structures of adenovirus 2 fiber message and the other late mRNAs. Cell 15:497–510. https://doi.org/10.1016/0092-8674(78)90019-3.
40. Yueh A, Schneider RJ. 1996. Selective translation initiation by ribosome jumping in adenovirus-infected and heat-shocked cells. Genes Dev 10:1557–1567. https://doi.org/10.1101/gad.10.12.1557.
41. Yueh A, Schneider RJ. 2000. Translation by ribosome shunting on adenovirus and hsp70 mRNAs facilitated by complementarity to 18S rRNA. Genes Dev 14:414–421. https://doi.org/10.1101/gad.14.4.414.
42. Knuckles P, Bühler M. 2018. Adenosine methylation as a molecular imprint defining the fate of RNA. FEBS Lett 592:2845–2859. https://doi.org/10.1002/1873-3468.13107.
43. Edupuganti RR, Geiger S, Lindeboom RGH, Shi H, Hsu PJ, Lu Z, Wang SY, Baltissen MPA, Jansen P, Rossa M, Muller M, Stunnenberg HG, He C, Carell T, Vermeulen M. 2017. N(6)-methyladenosine (m(6)A) recruits and repels proteins to regulate mRNA homeostasis. Nat Struct Mol Biol 24:870–878. https://doi.org/10.1038/nsmb.3462.
44. George J, Li Y, Kadamberi IP, Parashar D, Tsaih SW, Gupta P, Geethadevi A, Chen C, Ghosh C, Sun Y, Mittal S, Ramchandran R, Rui H, Lopez-Berestein G, Rodriguez-Aguayo C, Leone G, Rader JS, Sood AK, Dey M, Pradeep S, Chaluvally-Raghavan P. 2021. RNA-binding protein FXR1 drives cMYC translation by recruiting eIF4F complex to the translation start site. Cell Rep 37:109934. https://doi.org/10.1016/j.celrep.2021.109934.
45. McClure JJ, Palanisamy V. 2019. Muscle-specific FXR1 isoforms in squamous cell cancer. Trends Cancer 5:82–84. https://doi.org/10.1016/j.trecan.2018.12.001.
46. Baquero-Perez B, Antanaviciute A, Yonchev ID, Carr IM, Wilson SA, Whitehouse A. 2019. The Tudor SND1 protein is an m(6)A RNA reader essential for replication of Kaposi's sarcoma-associated herpesvirus. Elife 8:e47261. https://doi.org/10.7554/eLife.47261.
47. Kim DY, Reynaud JM, Rasalouskaya A, Akhrymuk I, Mobley JA, Frolov I, Frolova EI. 2016. New World and Old World alphaviruses have evolved to exploit different components of stress granules, FXR and G3BP proteins, for assembly of viral replication complexes. PLoS Pathog 12:e1005810. https://doi.org/10.1371/journal.ppat.1005810.
48. Soto-Acosta R, Xie X, Shan C, Baker CK, Shi PY, Rossi SL, Garcia-Blanco MA, Bradrick S. 2018. Fragile X mental retardation protein is a Zika virus restriction factor that is antagonized by subgenomic flaviviral RNA. Elife 7:e39023. https://doi.org/10.7554/eLife.39023.
49. Leong K, Berk AJ. 1986. Adenovirus early region 1A protein increases the number of template molecules transcribed in cell-free extracts. Proc Natl Acad Sci U S A 83:5844–5848. https://doi.org/10.1073/pnas.83.16.5844.
50. Jehung JP, Kitamura T, Yanagawa-Matsuda A, Kuroshima T, Towfik A, Yasuda M, Sano H, Kitagawa Y, Minowa K, Shindoh M, Higashino F. 2018. Adenovirus infection induces HuR relocalization to facilitate virus replication. Biochem Biophys Res Commun 495:1795–1800. https://doi.org/10.1016/j.bbrc.2017.12.036.
51. Michaels MG, Ison M, Green M. 2016. Adenovirus infection in solid organ transplantation, p 623–629. *In* Ljungman P, Snydman D, Boeckh M (ed), Transplant infection, 4th ed. Springer International Publishing, Cham, Switzerland.
52. Inturi R, Jemth P. 2021. CRISPR/Cas9-based inactivation of human papillomavirus oncogenes E6 or E7 induces senescence in cervical cancer cells. Virology 562:92–102. https://doi.org/10.1016/j.virol.2021.07.005.
53. Inturi R, Kamel W, Akusjarvi G, Punga T. 2015. Complementation of the human adenovirus type 5 VA RNAI defect by the Vaccinia virus E3L protein and serotype-specific VA RNAIs. Virology 485:25–35. https://doi.org/10.1016/j.virol.2015.07.002.
54. Komatsu T, Dacheux D, Kreppel F, Nagata K, Wodrich H. 2015. A method for visualization of incoming adenovirus chromatin complexes in fixed and living cells. PLoS One 10:e0137102. https://doi.org/10.1371/journal.pone.0137102.